Temperature-Dependent Polarization Characteristics of Composite-Resonator Vertical-Cavity Lasers

Daniel M. Grasso, *Student Member, IEEE,* and Kent D. Choquette, *Fellow, IEEE*

***Abstract*—We investigate the output characteristics from 10 °C to 160 °C of a monolithic dual-resonator vertical-cavity laser composed of three distributed Bragg reflector mirrors that separate two nominally identical optical cavities. The light output from the top ion-implanted cavity under forward bias is partitioned into two orthogonal polarizations of the fundamental transverse mode. A reverse bias of sufficient magnitude applied to the bottom oxide cavity causes the abrupt suppression of the dominant polarization and simultaneous emergence of the orthogonal polarization, consistent with wavelength dependent electroabsorptive loss in the reverse biased quantum wells of the oxide-confined cavity. We calculate the internal loss as a function of reverse bias and temperature, and characterize the polarization properties of the device based on the temperature dependence of the laser output. The polarization switching is consistent with increasing absorption with increasing temperature and decreasing absorption at longer wavelengths.**

***Index Terms*—Composite resonator, coupled cavity, polarization switching, vertical-cavity surface-emitting laser (VCSEL).**

I. Introduction

VERTICAL-CAVITY surface-emitting lasers (VCSELs) offer many advantages over Fabry–Perot edge-emitting lasers, including inherent high-speed operation and low threshold currents [1], [2]. However, with its typically isotropic transverse cavity geometry, the VCSEL light output is a superposition of two orthogonal polarizations for each transverse mode [3]. The two polarizations are usually found to lase at slightly different frequencies because of several factors. These include unintentional crystal strain induced during fabrication and electrooptic birefringence resulting from the built-in electric field in the structure [4]. In addition, the partitioning of the laser power into the two polarizations can be unequal and influenced by the relative spectral overlap with the temperature-dependent material gain [5], [6] and optical loss [7]. There has been considerable work in the area of polarization modulation and switching in VCSELs. Polarization switching has been achieved through a variety of techniques, including anisotropic cavity geometries [8], an external cavity with feedback [9], and optical injection [10].

In this work, we report the output characteristics under continuous-wave (CW) operation of a VCSEL with two optically coupled, electrically independent cavities. This structure will be referred to as a composite-resonator vertical-cavity laser (CRVCL) [11], [12]. The additional optical cavity can provide gain or loss to the coupled structure, depending on the biasing conditions [13]. In addition, polarization switching in CRVCLs has been reported under both pulsed and CW operation [14], [15]. We characterize the polarization properties of the CRVCL output, which can be modified by applying a reverse bias to one of the cavities. We also examine the temperature dependence of the laser output and polarization. The VCSEL structure and experimental setup are described in Section II. In Section III the polarization characteristics and temperature dependence are discussed. The paper concludes with potential applications for the CRVCL.

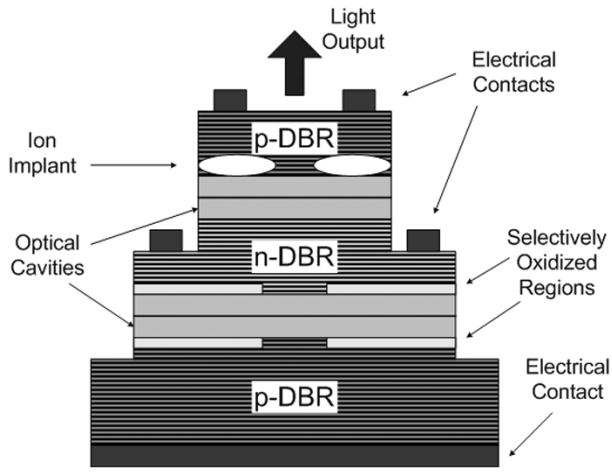

Fig. 1. Device structure for composite-resonator vertical-cavity laser.

II. Device Structure and Experiment

The device characterized in this work is a CRVCL with dual one-wavelength thick optical cavities, each of which contain five GaAs quantum wells (QWs). A schematic is shown in Fig. 1. The CRVCL is grown by metalorganic vapor phase epitaxy, and is composed of a monolithic bottom distributed Bragg reflector (DBR) with 35 periods, a middle DBR with 14.5 periods, and a top DBR with 21 periods. The CRVCL has two longitudinal resonances which can potentially lase [11], and the number of middle DBR pairs is chosen to determine the spectral splitting between these modes. The top cavity is transversely defined using ion implantation, with a current injection aperture diameter of 6 μm. The bottom cavity is defined using selective oxidation, and has an oxide aperture of approximately 10 μm $\times$ 10 μm. The device is fabricated in a double mesa structure to permit independent electrical injection into either cavity. The apertures of the top and bottom cavities are nominally aligned. The light output versus current

Manuscript received September 13, 2004; revised October 12, 2004. This work was supported in part by the National Science Foundation under Grant 0121662.

The authors are with the Department of Electrical and Computer Engineering, University of Illinois at Urbana–Champaign, Urbana, IL 61801 USA (e-mail: grasso@uiuc.edu).

Digital Object Identifier 10.1109/JQE.2004.840077

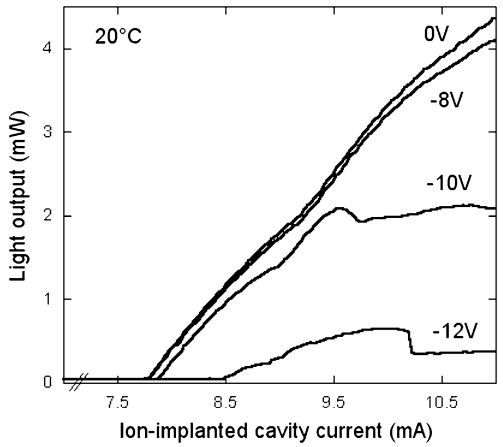

Fig. 2. Unpolarized room-temperature light output characteristics for current sweep in ion-implanted cavity. Oxide-confined cavity biases are labeled on curves.

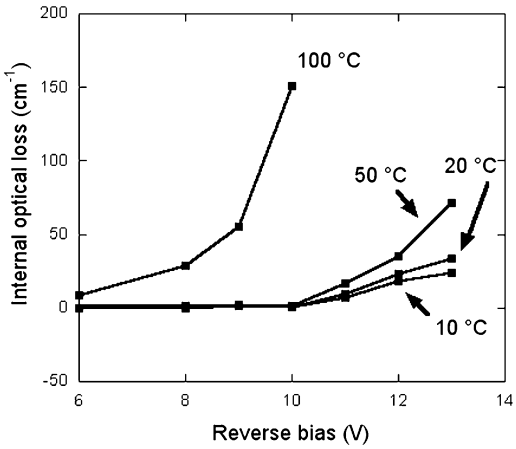

Fig. 3. Calculated internal loss in the CRVCL versus reverse bias in the oxide-confined cavity.

characteristics of the top ion-implanted cavity were measured by on-wafer probing using a semiconductor parameter analyzer, with the oxide-confined cavity simultaneously biased with a precision voltage source. In this work, we apply a reverse bias to the electrical junction of the oxide-confined cavity, and examine the effects on the laser emission. The light was captured with a Si photodetector, and the polarizations were distinguished with a linear polarizer. The spectral output of the device was examined using an optical spectrum analyzer with a resolution bandwidth of approximately 0.06 nm. The ambient substrate temperature was varied from 10 °C to 160 °C using a temperature-controlled probe station.

III. Output Characteristics

A. Electroabsorptive Loss in the Oxide-Confined Cavity

Fig. 2 shows the unpolarized, room temperature CW light output versus injection current only into the top ion-implanted cavity with various values of reverse bias applied to the bottom oxide-confined cavity. The reverse breakdown voltage of the electrical junction in the oxide-confined cavity is larger than -15 V over the entire temperature range studied. In all our measurements the reverse bias applied is less than this value, so that the p-n junction of the oxide-confined cavity is never in the current avalanche breakdown regime. An increase in reverse bias applied to the oxide-confined cavity causes an increase in threshold current and a decrease in differential slope efficiency, as apparent in Fig. 2. In the CRVCL biased under these conditions, the internal loss α_i has two components. The first is due to distributed optical losses such as free-carrier absorption and scattering in the DBR mirrors. This component is always present, and depends on temperature [16] but not on the biasing condition in the oxide-confined cavity. The second component is due to electroabsorptive loss in the reverse biased QWs of the oxide-confined cavity [15]. For a VCSEL operating above threshold and before thermal rollover, the light output P is approximated by

$$P = \frac{\hbar\omega}{q}\eta_i \frac{\alpha_m}{\alpha_i + \alpha_m}(I - I_{\rm th}) \tag{1}$$

where I is the injection current, $I_{\rm th}$ is the threshold current, η_i is the internal quantum efficiency, $\hbar\omega$ is the photon energy, q is the electron charge, and α_i and α_m are the internal and mirror losses, respectively. From (1), we can solve for the internal loss, which we write as $\alpha_i(V_{\rm rev})$ to show the explicit dependence on the reverse bias $V_{\rm rev}$ of the oxide-confined cavity:

$$\alpha_i(V_{\rm rev}) = \frac{\hbar\omega\eta_i\alpha_m(I - I_{\rm th})}{qP} - \alpha_m. \tag{2}$$

We have repeated the measurements shown in Fig. 2 at elevated temperatures. Using this data and (2), we calculate the change in internal loss as

$$\Delta\alpha = \alpha_i(V_{\rm rev}) - \alpha_{\rm min} \tag{3}$$

where $\alpha_{\rm min}$ is the minimum value of internal loss determined at each temperature.

Fig. 3 shows the change in internal loss versus reverse bias in the oxide-confined cavity for various temperatures. In this calculation, we assume an internal quantum efficiency of unity, and neglect the decrease in η_i with increasing temperature. The effective longitudinal cavity length of approximately 3 μm is measured from the output of a one-dimensional DBR simulation, and is taken as the $1/e$ point of the longitudinal electric field. From [17], we use

$$R = \frac{1 - \left(\frac{n_1}{n_2}\right)^{2m}}{1 + \left(\frac{n_1}{n_2}\right)^{2m}} \tag{4}$$

to calculate the DBR mirror reflectivities with high (low) index layers having refractive index of $n_1(n_2)$ and m periods. We ignore the coupling effects of the middle mirror and the thermal dependence of the semiconductor refractive index for this calculation. With $m_{\rm top} = 19$ pairs, $m_{\rm bottom} = 35$ pairs, and a DBR pair composition of $Al_{0.92}Ga_{0.08}As$–$Al_{0.16}Ga_{0.84}As$, the reflectivity of the top and bottom mirrors is approximately 99.2% and 99.99%, respectively. For each case, the internal loss does not change significantly until approximately -8 V, which is consistent with the output characteristics observed at 20 °C in Fig. 2. In addition, we find that the temperature dependence

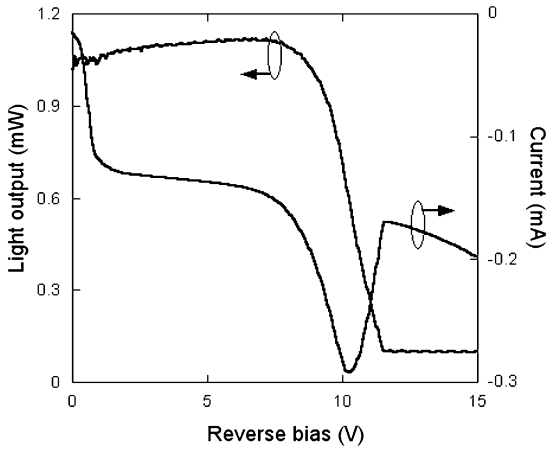

Fig. 4. Unpolarized light output from ion-implanted cavity and current in oxide-confined cavity versus reverse bias in oxide-confined cavity.

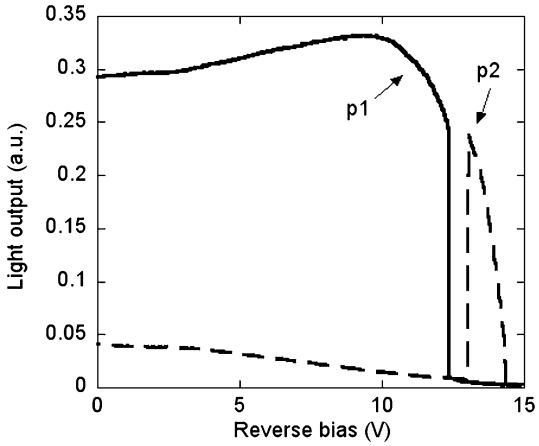

Fig. 5. Polarization-resolved light output from ion-implanted cavity versus reverse bias in oxide-confined cavity.

of the electroabsorption is nonlinear and increases dramatically above 50 °C. Although free-carrier absorption is dependent on both wavelength and temperature, the dominant loss mechanism under the reverse biasing conditions studied is quantum-well absorption. The large increase in internal loss with increasing temperature is consistent with previous work [16]. In the next section, we show that the wavelength dependence of the electroabsorptive loss dominates the polarization partitioning of the laser output.

B. Polarization of Laser Output

Fig. 4 shows the unpolarized light output of the device for approximately 8 mA of current injected into the top ion-implanted cavity and current in the oxide-confined cavity versus reverse bias applied to the oxide-confined cavity. Under these conditions, the output of the device is both single longitudinal and single transverse mode, with $\lambda \approx 900$ nm, regardless of the polarization. Similar to a conventional VCSEL, the emission is into two orthogonal linear polarizations whose absolute orientation is determined by factors such as crystal strain. This output represents a significant red shift from the peak of the material gain, which is nominally ≤ 850 nm for the GaAs QWs. The detuning is important for the analysis to follow. The light output in Fig. 4 is consistent with previous reports on a CRVCL with a bulk GaAs absorber as a second cavity [11], as well as integrated QW modulators in VCSELs [18]. The reverse bias current is apparently composed of two parts. The first is due to intrinsic carriers generated within the depletion region or minority carriers that diffuse to the junction and are collected [19]. The second component is due to electron-hole pairs that are optically generated through absorption of the laser emission. The large increase in the reverse current observed between -8 and -12 V in Fig. 4 occurs at the same bias conditions as the decrease (and eventual extinction) of light from the ion-implanted cavity. Once this emission is extinguished, the absorption component of the reverse current is no longer present and follows the previous functional dependence.

Fig. 5 shows an example of the light output versus reverse bias with the two orthogonal linear polarizations, p1 and p2, resolved. This measurement is taken at 20 °C with 8 mA of current injected into the ion-implanted cavity. When the oxide-confined cavity is open circuited, the output of the ion-implanted cavity lases simultaneously in two orthogonal linear polarization states, with the p1 polarization dominant. As the reverse bias in the oxide-confined cavity is initially increased, the majority of the light is maintained in the dominant p1 polarization, although the partitioning changes slightly. However, at approximately -13 V there is an abrupt switch and the p1 state is suppressed in favor of the orthogonal polarization p2 [15]. Eventually as the reverse bias is increased to -15 V, both p1 and p2 states are extinguished. Small changes in the ion-implanted cavity current near 8 mA do not cause a polarization switch if the reverse bias is held constant. For a given device, this switch occurs at slightly different values of reverse bias for repeated sweeps of voltage. This is the cause of the small gap between the turn off of the p1 state and the turn on of the p2 state in Fig. 3, as well as the small shift in voltage between the light output shown in Figs. 4 and 5. The reverse bias required to produce the polarization switch varies by less than 10% between different devices measured. In addition, we have measured devices where the switch occurs from p2 to p1, indicating no evidence of a systematic preferred initial polarization state across the sample.

Fig. 6 shows the wavelengths of the p1 and p2 polarizations versus reverse bias in the oxide-confined cavity. The initial apparent birefringence is smaller than the resolution bandwidth of the optical spectrum analyzer. Near the reverse bias corresponding to the polarization switch, however, there is an increase in the birefringence between p1 and p2 that is larger than the experimental error. The measurements of birefringence taken in [14] under pulsed operation showed no dependence on the voltage applied; therefore, the mechanism causing the switch here is different. The increase in wavelength splitting between p1 and p2 is consistent with the electrooptic effect, which is known to cause birefringence in VCSELs [4].

It is also notable that near the polarization switch, the orthogonal polarization p2 shifts to a longer wavelength than p1. Both of these trends have been observed from several CRVCL devices. Since both polarization modes are significantly red shifted with respect to the material gain, the mode with shorter

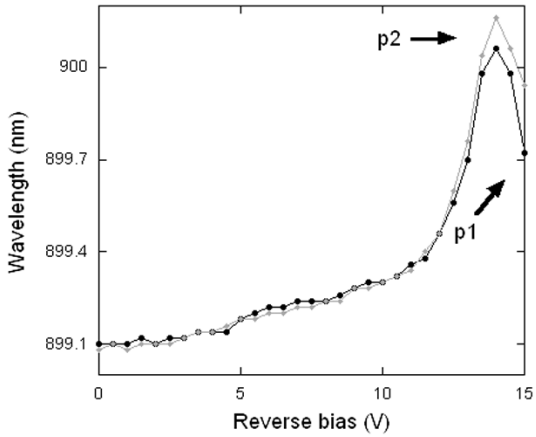

Fig. 6. Spectral evolution versus reverse bias in oxide-confined cavity.

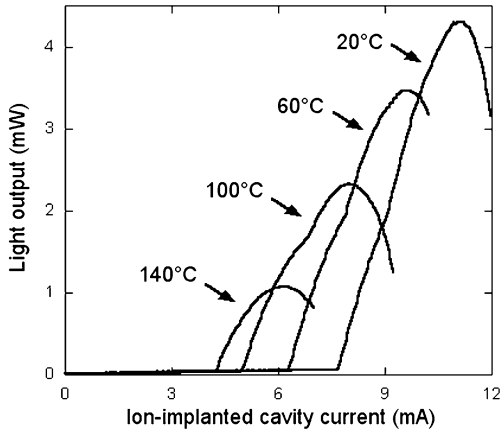

Fig. 7. Light output from ion-implanted cavity for various temperatures.

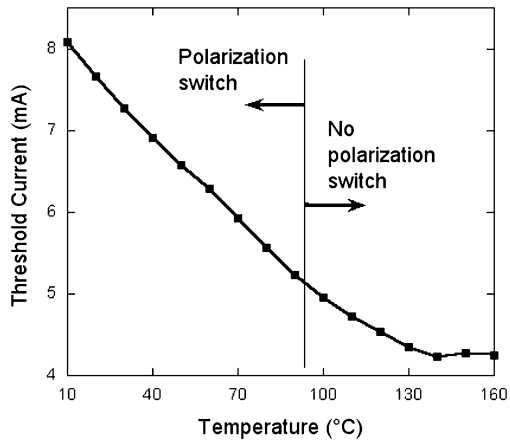

Fig. 8. Threshold current measured in ion-implanted cavity for various temperatures.

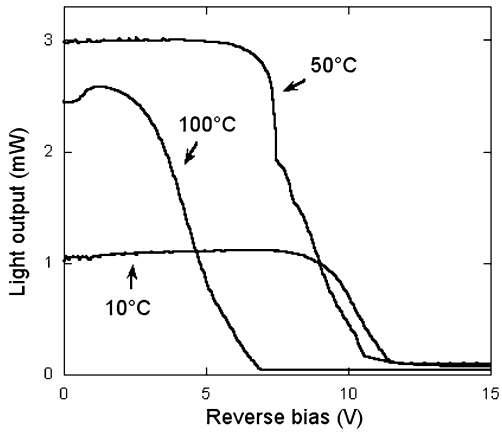

Fig. 9. Unpolarized light output from ion-implanted cavity versus reverse bias in oxide-confined cavity for various temperatures.

wavelength should have more available gain. Furthermore, with heating the peak of the material gain will shift to longer wavelengths [5]. Therefore, we do not believe that the polarization switch is caused by the relative spectral overlap of p1 and p2 with the material gain, where the spectral overlap may be changing with reverse bias in the oxide-confined cavity.

The data in Figs. 5 and 6 is consistent with the general trend of decreasing absorption coefficient, α, for wavelengths longer than the bandgap of bulk GaAs [20]. Herzinger *et al.* calculated the value $\Delta\alpha/\Delta\lambda \sim 1$ to 5 cm^{-1}/nm, which would produce sufficient excess loss for the shorter wavelength mode to induce a polarization switch (especially given the increased birefringence near -13 V in Fig. 6). Therefore, with increasing reverse bias, the polarization with longer wavelength will encounter less electroabsorption and therefore become the dominant lasing mode, as observed in Fig. 5.

As the temperature is increased in a VCSEL, the material gain and cavity resonance both shift to longer wavelengths, although the material gain shift is much larger [5]. If the temperature is increased enough, the cavity resonance will become completely misaligned spectrally with the material gain, and the laser output will be extinguished. Fig. 7 shows the output characteristics of the CRVCL at various temperatures up to 160 °C with the ion-implanted cavity forward biased, and the oxide-confined cavity open circuited. This broad range in operating temperature is partly due to the large offset of the cavity resonance; the spectral alignment with the material gain becomes better as the temperature is increased.

Fig. 8 shows a plot of the CRVCL threshold current over the temperature range considered. The general trend of decreasing threshold current with increasing temperature arises from the large spectral offset between the laser gain and the cavity resonance at room temperature. As the sample is heated, the improved spectral alignment corresponds to a decrease in the current required to reach threshold, as seen in Figs. 7 and 8.

We observe no polarization switch with increasing reverse bias for temperatures greater than approximately 100 °C. For sufficiently high temperature, the polarization with the longer wavelength has both better alignment with the material gain and reduced loss from electroabsorption. These two factors should imply suppression of the polarization switch, in agreement with our observations in Fig. 8.

Fig. 9 shows the light output from the ion-implanted cavity versus reverse bias in oxide-confined cavity for various temperatures. As the temperature is increased, the laser output is extinguished at smaller values of reverse bias. We observe that the polarization switch always occurs near the reverse bias where the total light output also starts to decrease. This implies that the polarization switch is occurring at a lower value of reverse bias

with increasing temperature. The data shown in Fig. 8 is consistent with the increased internal loss at higher temperatures shown in Fig. 3.

IV. Conclusion

In summary, we have reported the CRVCL polarization characteristics under CW operation with one cavity biased near threshold and the other reverse biased. The laser emission in this reverse biased operation is dominated by the wavelength and temperature dependence of the internal loss in the device, which is mainly due to QW absorption. Our results are consistent with increasing absorption with increasing temperature and decreasing absorption at longer wavelengths, both in agreement with previous reports for edge-emitting structures. The polarization switching of light in a CRVCL provides a novel method for controlling the laser output since the switch is created by an electric field external to the lasing cavity.

The CRVCL may be useful as an optical source in polarization-sensitive applications.

Acknowledgment

The authors would like to thank A. Allerman and K. Geib at Sandia National Laboratories, Albuquerque, NM, for providing the CRVCL samples.

References

[1] K. D. Choquette and K. M. Geib, "Fabrication and performance of vertical-cavity surface-emitting lasers," in *Vertical-Cavity Surface-Emitting Lasers*, C. Wilmsen, H. Temkin, and L. Coldren, Eds. Cambridge, U.K.: Cambridge Univ. Press, 1999, pp. 193–232.

[2] F. S. Choa, Y. H. Lee, T. L. Koch, C. A. Burns, B. Tell, J. L. Lewell, and R. E. Leibenguth, "High speed modulation of vertical-cavity surface-emitting lasers," *IEEE Photon. Technol. Lett.*, vol. 3, no. 8, pp. 697–697, Aug. 1991.

[3] K. D. Choquette, D. A. Ritchie, and R. E. Leibenguth, "Temperature dependence of gain-guided vertical-cavity surface-emitting lasers," *Appl. Phys. Lett.*, vol. 64, pp. 2062–2062, 1994.

[4] M. P. van Exter, A. K. Jansen van Doorn, and J. P. Woerdman, "Electro-optic effect and birefringence in semiconductor vertical-cavity lasers," *Phys. Rev. A*, vol. 56, pp. 845–845, 1997.

[5] K. D. Choquette, D. A. Ritchie, and R. E. Leibenguth, "Temperature dependence of gain-guided vertical-cavity surface-emitting lasers," *Appl. Phys. Lett.*, vol. 64, pp. 2062–2062, 1994.

[6] K. D. Choquette, R. P. Schneider Jr, K. L. Lear, and R. E. Leibenguth, "Gain-dependent polarization properties of vertical-cavity lasers," *IEEE J. Sel. Top Quantum Electron.*, vol. 1, no. 2, pp. 661–661, Jun. 1995.

[7] B. Ryvkin, K. Panajotov, A. Georgievski, J. Danckaert, M. Peeters, G. Verschaffelt, H. Thienpont, and I. Veretennic, "Effect of photon-energy-dependent loss and gain mechanisms on polarization switching in vertical-cavity surface-emitting lasers," *J. Opt. Soc. Amer. B*, vol. 16, pp. 2106–2106, 1999.

[8] K. D. Choquette, K. L. Lear, R. E. Leibenguth, and M. T. Asom, "Polarization modulation of cruciform vertical-cavity laser diodes," *Appl. Phys. Lett.*, vol. 64, pp. 2767–2767, 1994.

[9] S. Jiang, Z. Pen, M. Dagenais, R. A. Morgan, and K. Kojima, "High-frequency polarization self-modulation invertical-cavity surface-emitting lasers," *Appl. Phys. Lett.*, vol. 63, pp. 3545–3545, 1993.

[10] K. Panajotov, F. Berghmans, M. Peeters, G. Verschaffelt, J. Danckaert, I. Veretennicoff, and H. Thienpont, "Data transparent reconfigurable optical interconnections using polarization switching in VCSELs induced by optical injection," *IEEE Photon. Technol. Lett.*, vol. 11, no. 8, pp. 985–985, Aug. 1999.

[11] R. P. Stanley, R. Houdre, U. Oesterle, M. Ilegems, and C. Weisbuch, "Coupled semiconductor microcavities," *Appl. Phys. Lett.*, vol. 65, pp. 2093–2093, 1994.

[12] A. J. Fischer, K. D. Choquette, W. W. Chow, H. Q. Hou, and K. M. Geib, "Coupled-resonator vertical-cavity laser diode," *Appl. Phys. Lett.*, vol. 75, no. 19, pp. 3020–3020, 1999.

[13] D. M. Grasso and K. D. Choquette, "Threshold and modal characteristics of composite-resonator vertical-cavity lasers," *IEEE J. Quantum Electron.*, vol. 39, no. 12, pp. 1526–1526, Dec. 2003.

[14] V. Badilita, J.-F. Carlin, M. Ilegems, M. Brunner, G. Verschaffelt, and K. Panajotov, "Control of polarization switching in vertical coupled-cavities surface-emitting lasers," *IEEE Photon. Technol. Lett.*, vol. 16, no. 2, pp. 365–365, Feb. 2004.

[15] D. M. Grasso and K. D. Choquette, "Polarization switching in composite-resonator vertical-cavity lasers," *Appl. Phys. Lett.*, vol. 83, pp. 5148–5148, 2003.

[16] V. Mikhaelashvili, N. Tessler, R. Nagar, G. Eisenstein, A. G. Dentai, S. Chandrasakhar, and C. H. Joyner, "Temperature dependent loss and overflow effects in quantum-well lasers," *IEEE Photon. Technol. Lett.*, vol. 6, no. 11, pp. 1293–1293, Nov. 1994.

[17] L. A. Coldren and S. W. Corzine, *Diode Lasers and Photonic Integrated Circuits*. New York: Wiley, 1995.

[18] S. Lim, J. Hudgings, L. Chen, G. Li, W. Yuen, K. Lau, and C. Chang-Hasnain, "Modulation of a vertical-cavity surface-emitting laser using an intracavity quantum-well absorber," *IEEE Photon. Technol. Lett.*, vol. 10, no. 3, pp. 319–319, Mar. 1998.

[19] B. G. Streetman and S. Banerjee, *Solid State Electronic Devices*. Upper Saddle River, NJ: Prentice-Hall, 2000.

[20] C. M. Herzinger, P. D. Swanson, T. K. Kang, T. M.Cockerill, L. M. Miller, M. E. Givens, T. A. DeTemple, J.J. Coleman, and J. P. Leburton, "Electroabsorption properties of a single GaAs quantum well," *Phys. Rev. B*, vol. 44, pp. 13 479–13 479, 1991.

Daniel M. Grasso (S'99) received the B.S. degrees in electrical engineering and mathematics from the State University of New York at Buffalo in 2000, and the M.S. degree in electrical engineering from the University of Illinois at Urbana-Champaign in 2002. He is currently working toward the Ph.D. degree in electrical engineering at the University of Illinois in the Photonic Device Research Group.

His research interests include fabrication and high-speed characterization of VCSELs and opto-electronic devices.

Kent D. Choquette (M'97–F'03) received the B.S. degrees in engineering physics and applied mathematics from the University of Colorado, Boulder, in 1984 and the M.S. and Ph.D. degrees in materials science from the University of Wisconsin, Madison, in 1985 and 1990, respectively.

In 1990, he held a postdoctoral appointment at AT&T Bell Laboratories, Murray Hill, NJ, and in 1993, he joined Sandia National Laboratories, Albuquerque, NM, where he was a Principal Member of Technical Staff. He became a Professor in the Electrical and Computer Engineering Department at the University of Illinois at Urbana–Champaign in 2000. His research group is centered around the design, fabrication, and characterization of vertical-cavity surface-emitting lasers (VCSELs), novel microcavity light sources, nanofabrication technologies, and hybrid integration techniques. From 2000 to 2002, he was a IEEE/LEOS Distinguished Lecturer. He has authored over 150 publications and three book chapters, and has presented numerous invited talks and tutorials on VCSELs.

Prof. Choquette has served as an Associate Editor of the IEEE Journal of Quantum Electronics, Guest Editor of IEEE Journal of Selected Topics in Quantum Electronics, and presently is an Associate Editor of the IEEE Photonic Technology Letters. He is a Fellow of IEEE/Lasers and Electro-Optics Society (LEOS) and a Fellow of the Optical Society of America (OSA).